

# A Case Study of the Effects of Aerosols on South China Convective Precipitation Forecast

yueya wang<sup>1</sup>, Zijing ZHANG<sup>1</sup>, Wing Sze Chow<sup>1</sup>, Zhe Wang<sup>2</sup>, Jian Zhen Yu<sup>3</sup>, Jimmy Chi-Hung Fung<sup>1</sup>, and Xiaoming Shi<sup>4</sup>

<sup>1</sup>Hong Kong University of Science and Technology

<sup>2</sup>copyright, serif The Hong Kong University of Science and Technology

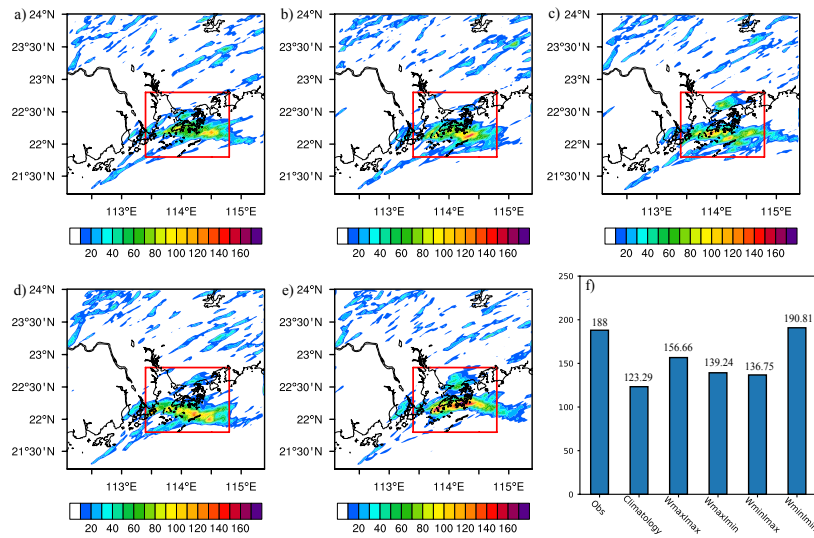
<sup>3</sup>The Hong Kong University of Science and Technology

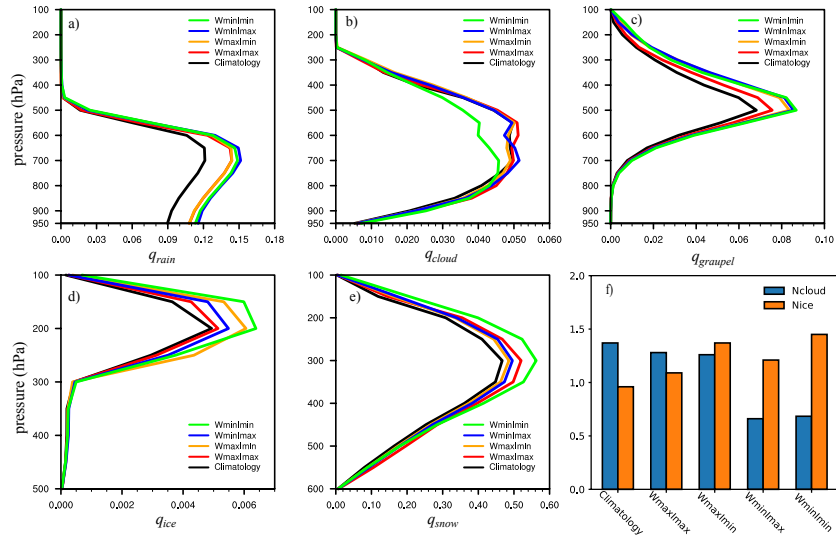
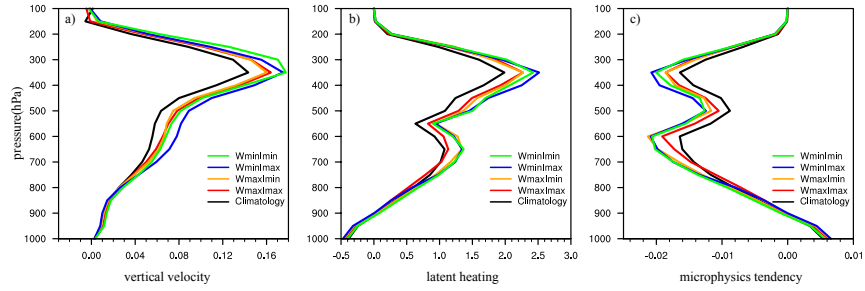
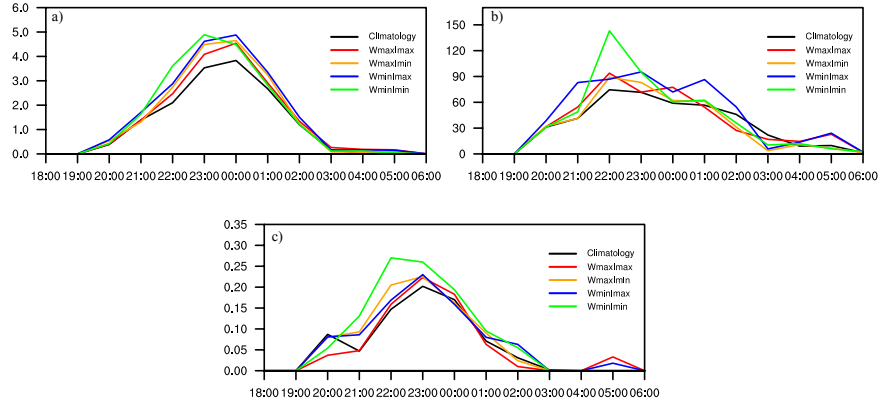
<sup>4</sup>Division of Environment and Sustainability, Hong Kong University of Science and Technology

January 3, 2023

## Abstract

Previous studies on South China's convective precipitation forecast focused on the effects of multi-scale dynamics and microphysics parameterizations. However, how the uncertainty in aerosol data might cause errors in quantitative precipitation forecast (QPF) has yet to be investigated. In this case study, we estimate the impact of aerosol uncertainties on the QPF for South China's severe convection using convection-permitting simulations. The variability range of aerosol concentrations is estimated with past observation for the pre-summer months. Simulation results suggest that the rainfall pattern and intensity change notably when aerosol concentrations are varied. The simulation with low aerosol concentrations produces the most intense precipitation, approximately 50% stronger than the high-concentration simulation. Decreasing aerosol hygroscopicity also increases precipitation intensity, especially in pristine clouds. The aerosol uncertainty changes alter the number of cloud condensation and ice nuclei, which modifies the altitude and amount of latent heating and thereby modulates convection.





# A Case Study of the Effects of Aerosols on South China Convective Precipitation Forecast

Yueya Wang<sup>1</sup>, Zijing Zhang<sup>1</sup>, Wing Sze Chow<sup>2</sup>, Zhe Wang<sup>1</sup>, Jian Zhen Yu<sup>1,2</sup>, Jimmy  
Chi-Hung Fung<sup>1,3</sup>, and Xiaoming Shi<sup>1</sup>

<sup>1</sup>Division of Environment and Sustainability, Hong Kong University of Science and Technology, Hong Kong, China

<sup>2</sup>Department of Chemistry, Hong Kong University of Science and Technology, Hong Kong, China

<sup>3</sup>Department of Mathematics, Hong Kong University of Science and Technology, Hong Kong, China

## Key Points:

- The pre-summer rainfall in South China is often caused by convection with low predictability.
- Convection-permitting simulations of a severe storm case were conducted with possible aerosol concentrations and properties scenarios.
- For this case study, lower concentrations of water- and ice-friendly aerosols lead to notably more vigorous convection and precipitation.

---

Corresponding author: Xiaoming Shi, [shixm@ust.hk](mailto:shixm@ust.hk)

**Abstract**

Previous studies on South China's convective precipitation forecast focused on the effects of multi-scale dynamics and microphysics parameterizations. However, how the uncertainty in aerosol data might cause errors in quantitative precipitation forecast (QPF) has yet to be investigated. In this case study, we estimate the impact of aerosol uncertainties on the QPF for South China's severe convection using convection-permitting simulations. The variability range of aerosol concentrations is estimated with past observation for the pre-summer months. Simulation results suggest that the rainfall pattern and intensity change notably when aerosol concentrations are varied. The simulation with low aerosol concentrations produces the most intense precipitation, approximately 50% stronger than the high-concentration simulation. Decreasing aerosol hygroscopicity also increases precipitation intensity, especially in pristine clouds. The aerosol uncertainty changes alter the number of cloud condensation and ice nuclei, which modifies the altitude and amount of latent heating and thereby modulates convection.

**Plain Language Summary**

Convective weather frequently happens in South China during the pre-summer season with limited forecast skills. Previous studies have investigated the impact of large-scale circulation, water vapor conditions, and complex topography in forming convective precipitation systems. However, how chemistry interacts with weather dynamics has yet to be investigated in the context of South China's convective weather. Aerosols can serve as cloud condensation nuclei (CCN) and ice nuclei (IN), and their concentration or property variation can affect various processes in cloud and precipitation formation. To estimate the impact of aerosol uncertainty on South China's pre-summer rainfall, we conducted simulations of a severe convection case with different aerosol concentrations and properties. We found that the typical aerosol concentration and property variability changed the convective system notably, which further influenced the rainfall pattern and intensity. The aerosols invigorate convection when they cause more latent heating or shift the vertical heating distribution upward. This work contributes to understanding the aerosol effects on convection and suggests the potential benefits of increasing aerosol observations in the future to improve the operational numerical forecast.

**1 Introduction**

Intense convection frequently occurs during the April-June (pre-summer) rainy season in South China and produces almost half the amount of local annual rainfall, and severe flooding resulting from extreme precipitation in this season often endangers the safety of lives and causes substantial economic losses (Luo et al., 2017). Previous studies examined the modulation of the pre-summer rainfall in South China from the perspectives of large-scale circulation, macro- and micro-scale cloud processes, and local dynamics (e.g., Luo et al., 2017; G. Chen et al., 2018; M. Li et al., 2022). It is found that a large fraction of the pre-summer rainfall is produced by convection in the warm sector region hundreds of kilometers ahead of a cold or quasi-stationary front. However, the convection initiation (CI), which depends on the multiscale interaction of atmospheric dynamics, is notoriously known for its relatively low predictability in the warm sector regions (Luo et al., 2017; Bai et al., 2021; Zhang et al., 2022). Therefore, the warm-sector CI is a major contributor to the errors in quantitative precipitation forecast (QPF) for the region. Recent studies revealed that a few factors, including low-level jets, small-scale variability of moisture pooling, and local orography together regulate the CI, rendering its accurate prediction very challenging (Du & Chen, 2018, 2019b; Bai et al., 2021).

Besides the complexity of dynamics, uncertainties in microphysics parameterizations can also strongly affect the prediction of the convective rainfall in the South China region. Qian et al. (2018) found that although using different microphysics schemes did not strongly affect CI, the movement and organization of simulated squall lines are sensitive to the variation of microphysics parameterizations. Yin et al. (2018) suggest that latent heating is an important factor in governing the intensity of convection, while rain evaporation is also suggested as a critical process due to its effect on regu-

64 lating cold pool intensity (Qian et al., 2018; Zhao et al., 2021; Zhou et al., 2022). Zhao et al. (2021)  
65 additionally highlighted the impact of the accurate and flexible representation of ice particle prop-  
66 erties on simulating the transition zone between convective and stratiform precipitation in a squall  
67 line.

68 However, how atmospheric chemistry, namely aerosols, may play a role in affecting the QPF  
69 in South China through interacting with cloud microphysics has not been quantitatively evaluated.  
70 A recent study based on radar and distrometer observations for South China suggests that raindrops  
71 in this region have sizes larger than the typical “maritime” regime but number concentrations higher  
72 than the typical “continental” regime (Yu et al., 2022). Such unique characteristics of hydrometers  
73 may reflect the complexity of the aerosol source and composition in this region due to its coastal  
74 location and the development of industries in South China (Wong et al., 2022). Aerosols play the  
75 roles of cloud condensation nuclei (CCN) and ice nuclei (IN), and therefore the variability of aerosol  
76 composition and concentration can directly change cloud characteristics and indirectly influence the  
77 radiation budget of the atmosphere, the accuracy of which is critical for successful climate modeling.  
78 Idealized numerical simulations have helped to make important progress on the interaction between  
79 aerosols and convective systems, but it is still unclear how relevant the uncertainties in aerosol in-  
80 formation are to the QPF in a particular region. This issue is partially a result of the complexity of  
81 aerosol-dynamics interaction depending on detailed characteristics of deep convection over differ-  
82 ent regions (Fan et al., 2016). The other factor is the idealized approach adopted by some previous  
83 studies, which often compare arbitrarily defined ‘pristine’ and ‘polluted’ conditions with the concen-  
84 tration of aerosols differing from a factor of ten to a few orders of magnitude (e.g., Q. Chen et al.,  
85 2019; Chang et al., 2021; Miyamoto, 2021). Researchers had to design their experiments in such an  
86 idealized way because of the lack of long-term concurrent observation of aerosol properties that can  
87 address the covariability of aerosols, dynamics, and thermodynamics (Fan et al., 2016). Here, we use  
88 available observations of aerosols properties in Hong Kong to estimate the range of their variabil-  
89 ity and employ the Weather Research and Forecast (WRF) model with the aerosol-aware Thompson  
90 microphysics scheme (Thompson & Eidhammer, 2014) to semi-quantitatively assess the impact of  
91 the uncertainties of aerosol information on the QPF of South China coastal region convection.

## 92 **2 Methods and Experiments**

### 93 **2.1 Case Description**

94 We conduct our experiments with the severe convective rainstorm case on June 27 and 28,  
95 2021, in Hong Kong. It is categorized as a “black rainstorm” (hourly rainfall exceeding 70mm)  
96 according to Hong Kong Observatory’s (HKO) rainstorm warning system. The heavy rainfall appears  
97 to be caused by a boundary layer jet (Supporting Fig. S1), which is often associated with warm  
98 sector convection (Du & Chen, 2019a). However, this case is not typical in that the cold front to the  
99 west of Hong Kong is weak, if not none (Supporting Fig. S1b). Although, the active southwesterly  
100 airstream does bring warm moist flow from the South China Sea to the coast of Guangdong. The  
101 precipitation was intense and persistent on the morning of June 28, and a black rainstorm warning  
102 was issued. Over 150 millimeters of rainfall were recorded at many observation stations. Numerical  
103 forecast underestimated the precipitation and led to a late issuing of the black rainstorm warning on  
104 the morning of June 28 (HKO, 2021).

### 105 **2.2 Experiment Design**

106 The simulation was configured with three nested domains with horizontal grid resolutions  
107 of 9km, 3km, and 1km, respectively, using the WRF model version 4.3.1 (Supporting Figure S1).  
108 The vertical direction has 51 levels up to the model top at 50hPa. Each simulation was run for 24  
109 hours, starting from 06 UTC on June 27, 2021. The Thompson aerosol-aware microphysics scheme  
110 (Thompson & Eidhammer, 2014) was employed in the simulations. The aerosols in the scheme are  
111 divided into water-friendly aerosols for cloud condensation nuclei (CCN) and ice-friendly aerosols  
112 for ice nuclei (IN). The CCN activation is based on a look-up table which is derived from the Köhler  
113 activation theory with a parcel model, and the IN-number concentration follows the parameterization

114 of DeMott et al. (2010). The water-friendly aerosol is comprised of sulfates, nitrate, sea salts, and  
 115 organic carbon, and the ice-friendly aerosol is primarily considered to be dust. The aerosol emissions  
 116 are simplified and represented based on the starting near-surface aerosol concentrations. The scheme  
 117 is a bulk microphysics scheme and has double moment ice and rain. Other model configuration de-  
 118 tails are shown in Supporting Table S1.

119 A set of simulations were run to test the impact of different aerosol states with varying water-  
 120 and ice-friendly aerosol concentrations on the cloud and precipitation development. The default  
 121 option for the aerosol-aware scheme is to use the climatological mean aerosol concentration derived  
 122 from the seven years (2001-2007) simulation of the Goddard Chemistry Aerosol Radiation and Trans-  
 123 port (GOCART) model (Colarco et al., 2010; Thompson & Eidhammer, 2014). Our simulation using  
 124 this default option is denoted as the ‘‘Climatology’’ experiment as a reference.

125 For sensitivity tests, we adjust the aerosol concentration based on the observed variability of  
 126 aerosols in Hong Kong. Observational aerosol data are available for April to June 2020 at the Tuen  
 127 Mun Air Quality Monitoring Station in Hong Kong (22°23'28.4" N, 113°58'37.1" E, 30 m above  
 128 ground level) (Wong et al., 2022). Since the observatory data is near the surface, the scale factor is  
 129 calculated with respect to the lowest level of the GOCART climatology data. The mass concentration  
 130 of chemical species, including  $\text{SO}_4^{2-}$ ,  $\text{NO}_3^-$ ,  $\text{Na}^+$ , organic carbon (OC) and Al were obtained every  
 131 three days. The number concentration of the water-friendly aerosol (including sulfates, nitrate, sea  
 132 salts, and organic carbon) and ice-friendly aerosol (i.e. dust) was calculated from the observation  
 133 of related ion mass concentration by assuming that the aerosol size distribution follows a lognormal  
 134 distribution. The characteristic diameter and geometric standard deviation from the analysis results  
 135 of Bian et al. (2014) were used, and we assumed the aerosols were externally mixed.

136 The three-month time series of the number concentration of those aerosols in the observa-  
 137 tion period are shown in Supporting Figure S2. In that period, the maximum values of the water-  
 138 and ice-friendly aerosol number concentrations are 0.818 and 0.795 times, respectively, of the GO-  
 139 CART climatological monthly mean value for the precipitation event; the minima are 0.045 and  
 140 0.080 times, respectively, of the GOCART value. We scale the aerosol data for entire simulation  
 141 domains with those factors to roughly represent the range of aerosol concentration variability in the  
 142 pre-summer season. By combing the maximum and the minimum of the aerosol number concentra-  
 143 tions, we obtain four different experiments denoted as ‘‘WmaxImax’’, ‘‘WmaxImin’’, ‘‘WminImax’’,  
 144 and ‘‘WminImin’’, where ‘‘W’’ and ‘‘I’’ indicate water-friendly and ice-friendly aerosols, respectively,  
 145 and ‘‘max’’ or ‘‘min’’ following ‘‘W’’ or ‘‘I’’ indicates the scaling factor corresponding to the maximum  
 146 or minimum bounds of the associated aerosol group.

147 In our analysis, it is found that OC dominates the number concentration of water-friendly  
 148 aerosols. Observation data (Bian et al., 2014) suggests the OC aerosol has a relatively large frac-  
 149 tion of mass in the smaller condensation mode, leading to the higher number concentration in the  
 150 calculation assuming aerosols are externally mixed. The relatively flat size distribution of the OC is  
 151 beneficial to CCN activation in that size is suggested to be more important than composition in deter-  
 152 mining CCN activity (Dusek et al., 2006; Moore et al., 2012). Additionally, even though most fresh  
 153 organic species are insoluble, the aged organic species coated by soluble species such as sulfuric acid  
 154 vapor are more hygroscopic and can be activated as CCN; some observational studies have found that  
 155 the carbonaceous species coupled with sulfate, nitrite, and ammonium account for a larger fraction  
 156 in the condensation mode aerosols with evenly size distribution (Furutani et al., 2008; Novakov &  
 157 Penner, 1993). To further evaluate the potential bias in our estimation with assumed external mix-  
 158 ing, we estimated the actual number concentration of aerosols in the condensation mode based on the  
 159 measurement by a Scanning Mobility Particle Sizer (SMPS) at HKUST. The SMPS data is for April  
 160 2021 and for the diameter range of 10 nm to 763 nm. Assuming the local size distribution of aerosols  
 161 is time-invariant, we can establish a relation between the condensation mode number concentration  
 162 and  $\text{PM}_{2.5}$  mass concentration. Applying this relationship to the  $\text{PM}_{2.5}$  data for April to June 2020  
 163 yields an estimation of condensation model number concentration for the period, which ranges be-  
 164 tween  $231 \text{ cm}^{-3}$  and  $4281 \text{ cm}^{-3}$ . This range is roughly consistent with our estimation, including all  
 165 sizes and assuming external mixing, which ranges from  $620 \text{ cm}^{-3}$  to  $5458 \text{ cm}^{-3}$ . Therefore, while the  
 166 external mixing state assumption used in our estimation is not the reality (Riemer et al., 2019), it is

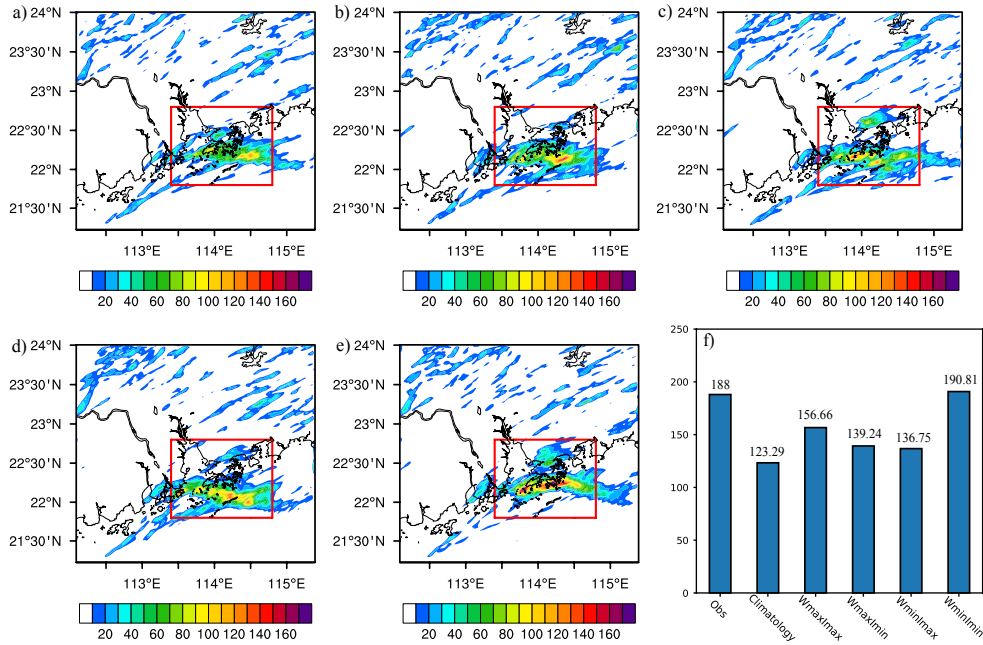


**Figure 1.** Accumulated precipitation from 12 UTC, 27 June to 06 UTC, 28 June of different experiments: (a) Climatology, (b) WmaxImax, (c) WmaxImin, (d) WminImax, (e) WminImin. The red box is marked as the core precipitation area in the domain. (f) is the maximal accumulated precipitation (mm) of the observation and the simulations over the core area.

167 reasonable to use those estimation results to approximate the variability of the number concentration  
 168 of water-friendly aerosols in this study.

### 169 3 Results

170 The accumulated precipitation in the simulations from 12 UTC, 27 June, to 06 UTC, 28 June, is  
 171 shown in Figure 1. We first compare the precipitation intensity and spatial pattern for all experiments.  
 172 From Figure 1a-e, it can be found that the precipitation patterns and intensity are different by chang-  
 173 ing the aerosol concentrations. All the simulations with reduced aerosol concentrations in the four  
 174 comparison experiments show more intense convection than the climatology simulation. The con-  
 175 vention of simulations with lower aerosol concentrations is stronger than those with higher aerosol  
 176 concentrations. For example, the precipitation of the WminImin (Figure 1e) is stronger than the  
 177 WmaxImax (Figure 1b). In addition, reducing the water-friendly and reducing ice-friendly aerosol,  
 178 the precipitation center of the WminImin simulation is located near Hong Kong, and the strongest  
 179 precipitation happened around Hong Kong Island, which matches the observation very well. Thus,  
 180 varying the aerosol conditions can change the CI, in this case, subtly. Furthermore, the intense con-  
 181 vention centers of the two Wmin simulations have larger cores than those in other experiments.

182 The maximum accumulated precipitation for all the experiments is shown in Figure 1f. The  
 183 four altered aerosol state simulations produce stronger precipitation maxima than the climatology  
 184 simulation, which underestimates precipitation compared with the observation. Furthermore, the  
 185 WminImin simulation with the minimal aerosol concentration predicted a maximum of approxi-  
 186 mately 190 mm, comparable with the observed rainfall of 180 mm. We noticed that when reducing  
 187 the water-friendly aerosols, the tendency of the maximum precipitation variation is different in the  
 188 Wmin and Wmax groups or the Imax and Imin groups. However, the comparison in Figure 1f is only

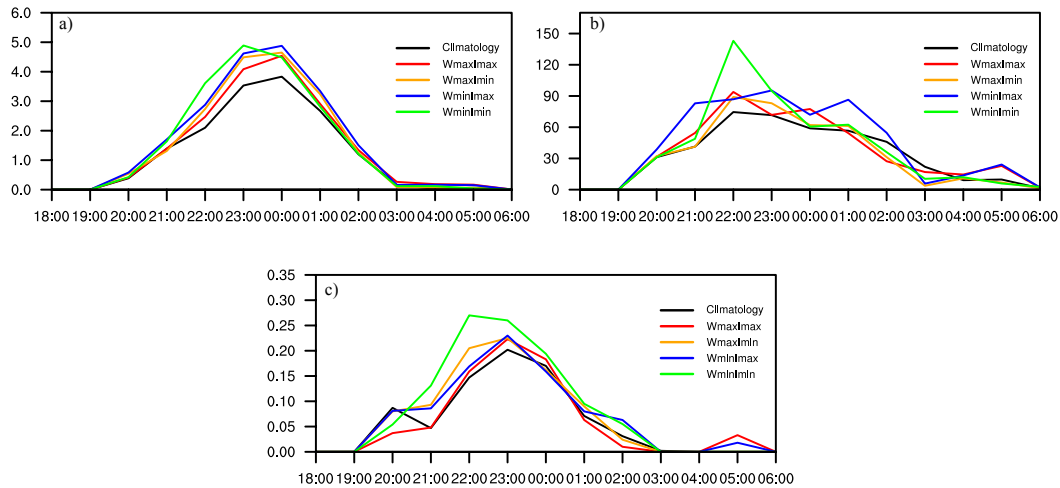


**Figure 2.** The hourly area average precipitation of the main region (red box in Figure 1), (b) the maximum hourly precipitation in the core area, and (c) the ratio of the area with hourly rainfall larger than 20mm to the total area of the core area.

189 based on the rainfall maximum point and misses the information over the whole precipitating area,  
 190 so below, we further analyze the precipitation over the main precipitation area (red box in Figure 1f).

191 The simulation results are evaluated based on the average (Figure 2a) and maximum precipi-  
 192 tation (Figure 2b) over the main impact area marked by the red box in Figure 1 from 19:00 UTC to  
 193 05:00UTC. The area average (Figure 2a) and the maximum (Figure 2b) precipitation intensity in the  
 194 two simulations with minimum water-friendly aerosol (Wmin) simulations are higher than in other  
 195 groups. The WminImax simulation has 30% more area-averaged precipitation than the Climatology  
 196 simulation, of which the precipitation intensity is the weakest during the entire process. The Wmin-  
 197 Imin simulation shows more extensive area-averaged precipitation at the early stage. Decreasing the  
 198 water (ice) aerosol concentration would lead to stronger precipitation in the core area under the high  
 199 ice-friendly (water-friendly) aerosol concentration condition. However, in the groups with minimum  
 200 water- or ice-friendly aerosol, the effect of reducing the other kind of aerosol is less significant. In  
 201 addition, the hourly precipitation maxima in the WminImin simulation are 140 mm, which is twice  
 202 larger than that of the Climatology simulation at 22:00 UTC. The maximum precipitation of Wmin-  
 203 Imax is also relatively higher. Figure 2c shows the percentage of the area where the rainfall is larger  
 204 than 20 mm in the main region. The heavy precipitation covered a larger area in the two simula-  
 205 tions with minimum ice-friendly aerosol concentration. The area covered by heavy rainfall in the  
 206 WminImin simulation is almost twice as large as the Climatology run for some short periods.

207 Therefore, the precipitation prediction differs notably for the varying aerosol states. Chang-  
 208 ing aerosol states influenced the temporal and spatial evolution of convective systems and thereby  
 209 affected the rainfall locations as well in the simulations. Higher rainfall intensity is found in the  
 210 minimal aerosol concentration simulation, which is more consistent with the observed intense rain-  
 211 fall. Lower water-friendly aerosol concentration expands the precipitation to a larger zone, and the  
 212 area average precipitation is relatively enhanced; reducing the ice-friendly aerosol can induce more  
 213 intense precipitation and maximum precipitation intensity.

214 We further examined the dynamic and microphysical conditions of different aerosol states to  
 215 understand the effects of aerosols. Figure 3 shows the vertical profiles of the averaged vertical ve-  
 216 locity from 21:00UTC to 02:00UTC over the main precipitation area. In the Wmin simulations, the  
 217 updraft velocity, latent heating, and microphysics tendency are more stronger. Likewise, the simula-

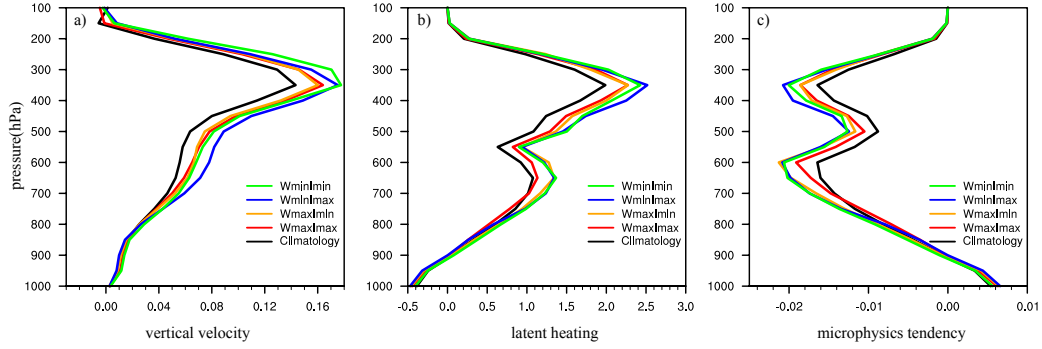


**Figure 3.** The vertical profiles of (a) vertical velocity ( $\text{m} \cdot \text{s}^{-1}$ ), (b) latent heating ( $\text{K} \cdot \text{d}^{-1}$ ) and (c) microphysics tendency for water vapor ( $10^{-3} \text{ s}^{-1}$  from 21:00 UTC to 02:00 UTC, averaged over the main precipitation area marked by the red box in Figure 1 for the five simulations.

218 tions in Imin groups also produce larger latent heating and more microphysics tendency than other  
 219 groups, despite the different water-friendly aerosol conditions. The updraft velocity of the Wmin-  
 220 Imax simulation is 60% (30%) larger than that in the Climatology simulation at 600hPa (300 hPa).  
 221 In addition, the latent heating and microphysics-induced tendency of the WminImin experiment is  
 222 also higher, which is 30% and 20% more than the Climatology simulation, respectively, both at low  
 223 and high-pressure levels. As a result, the precipitation intensity of the simulation with minimum  
 224 ice-friendly aerosols is higher than the other simulations in Figure 3. The difference in the profiles  
 225 reveals that, in this case, the environmental conditions are influenced by the aerosol concentration,  
 226 and reducing both kinds of aerosols can enhance the precipitation with higher updraft velocity,  
 227 more microphysical conversion and more latent heating. However, different mechanisms are involved here.  
 228 While the WminImin simulation exhibits stronger ascent in the upper troposphere, the WminImax  
 229 exhibits stronger ascent in the middle and lower troposphere and more latent heat release at the upper  
 230 levels.

231 We also compare the hydrometeor contents to evaluate the impact of the aerosol concentration  
 232 directly. Figure 4 shows the main precipitation region mean vertical profiles of the mass mixing  
 233 ratios (a-e) and vertically integrated number concentration (f) of the hydrometeors. The rainwater  
 234 (Figure 4a) is directly related to the precipitation. Figure 4a shows that the area-averaged rain mass  
 235 mixing ratio in the groups with reduced water-friendly aerosol concentration is higher than the clima-  
 236 tology group. We can see that the mass mixing ratio and number concentration of liquid cloud water  
 237 in Figure 4b and Figure 4f are significantly increased in the simulations with larger water-friendly  
 238 aerosol concentrations. The droplet size in those simulations then would be reduced, which can ex-  
 239 pand the cloud lifetime and decrease rainwater. Somewhat surprisingly, the graupel, snow, and ice  
 240 mass mixing ratio increased significantly in the experiments with minimum ice-friendly aerosols,  
 241 contributing to the precipitation increase. It appears that firstly the concentration of liquid cloud  
 242 droplets has an important impact on convection intensity by enhancing precipitation efficiency, thus,  
 243 the Wmin simulations have higher cloud ice number concentrations than Wmax simulations. Sec-  
 244 ondly, the decreased ice-friendly aerosol leads to higher cloud ice number concentration and further  
 245 precipitation particles due to the enhanced homogeneous process and more latent heat released at  
 246 upper levels, both of which can invigorate deep convection (Deng et al., 2018; Min et al., 2008).  
 247 Previous studies also confirmed that pristine convective clouds tend to develop a colder (higher) top  
 248 (R. Li et al., 2017). These factors lead to the result that the WminImin simulation produces the largest  
 249 maximum precipitation rate in Figure 2.

250 The hygroscopicity of the aerosols is also essential to the CCN activation, which further im-  
 251 pacts the convection evolution. These results are all based on the same default hygroscopicity param-  
 252 eter, 0.4, in the aerosol-aware Thompson scheme. However, the mixing state and chemical composi-

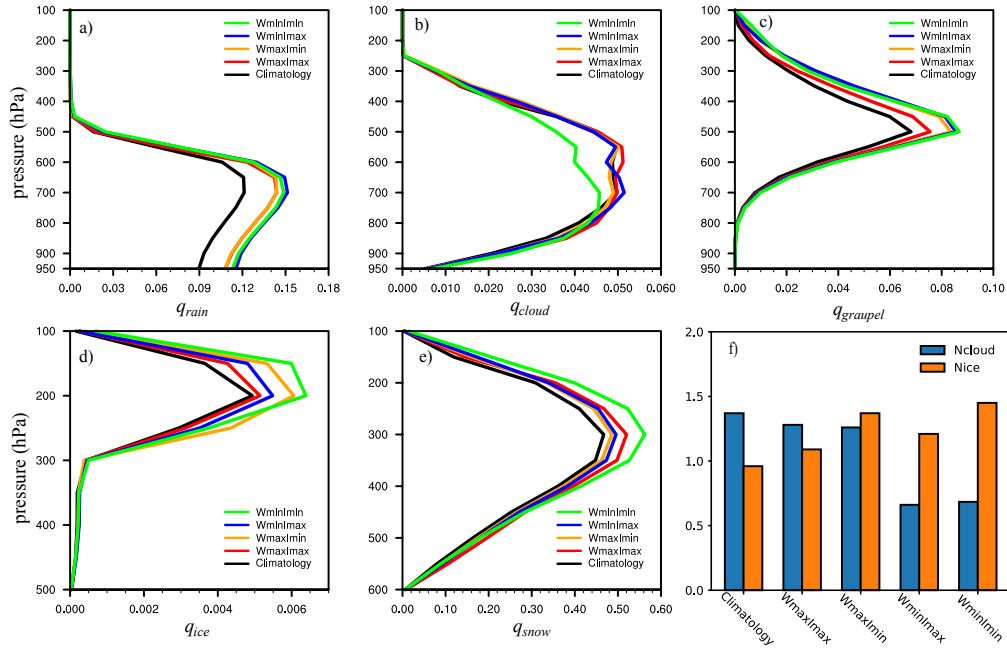


**Figure 4.** The vertical profiles of the mass mixing ratio ( $\text{g kg}^{-1}$ ) of the (a)  $q_{rain}$ , (b)  $q_{cloud}$ , (c)  $q_{graupel}$ , (d)  $q_{ice}$ , (e)  $q_{snow}$  averaged from 21:00UTC to 02:00UTC over the core area marked as the red box in Fig. 1 for the five simulations. (f) The core area mean of vertically integrated number concentration of liquid cloud ( $10^7 \text{ m}^{-2}$ , blue bar), ice cloud ( $10^5 \text{ m}^{-2}$ , red bar).

253 tion will change the aerosol hygroscopicity. Therefore, we further conducted another two simulations  
 254 under maximal and minimal aerosol conditions (WmaxImax and WminImin) following Yeung et al.  
 255 (2014) in which they suggested that the hygroscopicity of aerosol in Hong Kong is around 0.3. The  
 256 analyzed hygroscopicity is based on the observation of the Hong Kong supersite. The precipita-  
 257 tion simulation results are shown in Supporting Figure S3. We can see that the precipitation pattern  
 258 and location are similar under different aerosol concentration conditions. However, the precipitation  
 259 intensity is changed and is more sensitive to the hygroscopicity when the aerosol concentration is  
 260 minimal. Compared to the default hygroscopicity simulations, the maximal precipitation decreased  
 261 by 20% for WminImin and only 5% WmaxImax.

262 **4 Conclusion**

263 Aerosols serving as the cloud condensation nuclei and the ice nuclei are critical factors in  
 264 cloud formation. Aerosol concentration and composition variation can change the hydrometer size  
 265 and number concentration, cloud evolution, and furthermore, the dynamics and thermodynamics of  
 266 convection. In this study, we investigate the impact of aerosol concentration and property uncertainty  
 267 on the forecast of convective rainfall in South China with a case study. The aerosol-aware Thompson  
 268 microphysics scheme was used to evaluate the aerosol effect in convection-permitting WRF simula-  
 269 tions. We defined four aerosol concentration scenarios based on the observed variability of aerosols  
 270 in Hong Kong and included another reference run using the GOCART climatology data. All the simu-  
 271 lations based on observation aerosol concentrations, which are lower than GOCART climatology,  
 272 exhibited more intense convection and precipitation than the reference simulation. Decreasing the  
 273 hygroscopicity from the model default to a smaller value suggested by observation also increases the  
 274 predicted precipitation, but the change is more notable when aerosol concentrations are low.

275 The simulation with minimum water- and ice-friendly aerosol concentration conditions pro-  
 276 duced the most intense rainfall, which is close to the observed maximum value of the accumulated  
 277 rainfall and is approximately 50% higher than the prediction based on GOCART climatology. Thus,  
 278 the QPF of pre-summer is indeed sensitive to aerosol conditions for, at least, some intense convective  
 279 systems. For the case we studied, the reduction in CCN appears to enhance precipitation by increas-  
 280 ing droplet size and decreasing number concentration, which thereby reduces mid-level evaporation  
 281 and strengthens convection. The amount of IN appears to affect convection intensity by altering the  
 282 fraction of homogeneous and heterogeneous processes, the form of which becomes more dominant  
 283 in pristine clouds and deepens convection through the delayed release of latent heat at upper levels.

284 Our assessment is, admittedly, semi-quantitative, because, besides approximations used in our  
 285 aerosol data analysis, the microphysics scheme also has its own limitations (Morrison et al., 2020).  
 286 Additional complexity arises due to the dependency of aerosol effects on cloud systems and the en-  
 287 vironment, which may lead to different signs of precipitation changes in different cases when aerosol  
 288 conditions are varied (Fan et al., 2016). However, this preliminary evaluation suggests that accu-  
 289 rate aerosol measurement is essential for improving the numerical prediction of South China's pre-  
 290 summer convection. Fan et al. (2016) suggested that long-term concurrent measurements of aerosol  
 291 properties and meteorological fields are important for advancing our understanding and modeling  
 292 capability of aerosol-cloud interaction. Such observations, if available, are beneficial not only to  
 293 research efforts but also to operational weather forecasts.

## 294 References

- 295 Bai, L., Chen, G., Huang, Y., & Meng, Z. (2021). Convection initiation at a coastal rainfall hotspot  
 296 in south china: Synoptic patterns and orographic effects. *Journal of Geophysical Research:*  
 297 *Atmospheres*, *126*(24), e2021JD034642.
- 298 Bian, Q., Huang, X. H., & Yu, J. Z. (2014). One-year observations of size distribution characteristics  
 299 of major aerosol constituents at a coastal receptor site in hong kong—part 1: Inorganic ions and  
 300 oxalate. *Atmospheric Chemistry and Physics*, *14*(17), 9013–9027.
- 301 Chang, Y.-H., Chen, W.-T., Wu, C.-M., Moseley, C., & Wu, C.-C. (2021). Tracking the influence of  
 302 cloud condensation nuclei on summer diurnal precipitating systems over complex topography  
 303 in taiwan. *Atmospheric Chemistry and Physics*, *21*(22), 16709–16725.
- 304 Chen, G., Lan, R., Zeng, W., Pan, H., & Li, W. (2018). Diurnal variations of rainfall in surface and  
 305 satellite observations at the monsoon coast (south china). *Journal of Climate*, *31*(5), 1703–  
 306 1724.
- 307 Chen, Q., Yin, Y., Jiang, H., Chu, Z., Xue, L., Shi, R., ... Chen, J. (2019). The roles of mineral dust  
 308 as cloud condensation nuclei and ice nuclei during the evolution of a hail storm. *Journal of*  
 309 *Geophysical Research: Atmospheres*, *124*(24), 14262–14284.
- 310 Colarco, P., da Silva, A., Chin, M., & Diehl, T. (2010). Online simulations of global aerosol distribu-  
 311 tions in the nasa geos-4 model and comparisons to satellite and ground-based aerosol optical  
 312 depth. *Journal of Geophysical Research: Atmospheres*, *115*(D14).
- 313 DeMott, P. J., Prenni, A. J., Liu, X., Kreidenweis, S. M., Petters, M. D., Twohy, C. H., ... Rogers, D.  
 314 (2010). Predicting global atmospheric ice nuclei distributions and their impacts on climate.  
 315 *Proceedings of the National Academy of Sciences*, *107*(25), 11217–11222.
- 316 Deng, X., Xue, H., & Meng, Z. (2018). The effect of ice nuclei on a deep convective cloud in south  
 317 china. *Atmospheric Research*, *206*, 1–12.
- 318 Du, Y., & Chen, G. (2018). Heavy rainfall associated with double low-level jets over southern china.  
 319 part i: Ensemble-based analysis. *Monthly Weather Review*, *146*(11), 3827–3844.
- 320 Du, Y., & Chen, G. (2019a). Climatology of low-level jets and their impact on rainfall over southern  
 321 china during the early-summer rainy season. *Journal of Climate*, *32*(24), 8813–8833.
- 322 Du, Y., & Chen, G. (2019b). Heavy rainfall associated with double low-level jets over southern  
 323 china. part ii: Convection initiation. *Monthly Weather Review*, *147*(2), 543–565.
- 324 Dusek, U., Frank, G., Hildebrandt, L., Curtius, J., Schneider, J., Walter, S., ... others (2006).  
 325 Size matters more than chemistry for cloud-nucleating ability of aerosol particles. *Science*,  
 326 *312*(5778), 1375–1378.

- 327 Fan, J., Wang, Y., Rosenfeld, D., & Liu, X. (2016). Review of aerosol–cloud interactions: Mechanisms, significance, and challenges. *Journal of the Atmospheric Sciences*, *73*(11), 4221–4252.
- 328
- 329 Furutani, H., Dall’osto, M., Roberts, G. C., & Prather, K. A. (2008). Assessment of the relative importance of atmospheric aging on ccn activity derived from field observations. *Atmospheric Environment*, *42*(13), 3130–3142.
- 330
- 331
- 332 HKO. (2021). *Hong kong observatory*. Retrieved October 9, 2022, from <https://www.hko.gov.hk/en/wxinfo/pastwx/mws2021/mws202106.htm>.
- 333
- 334 Li, M., Luo, Y., & Min, M. (2022). Characteristics of pre-summer daytime cloud regimes over coastal south china from the himawari-8 satellite. *Advances in Atmospheric Sciences*, 1–16.
- 335
- 336 Li, R., Dong, X., Guo, J., Fu, Y., Zhao, C., Wang, Y., & Min, Q. (2017). The implications of dust ice nuclei effect on cloud top temperature in a complex mesoscale convective system. *Scientific Reports*, *7*(1), 1–9.
- 337
- 338
- 339 Luo, Y., Zhang, R., Wan, Q., Wang, B., Wong, W. K., Hu, Z., ... others (2017). The southern china monsoon rainfall experiment (scmrex). *Bulletin of the American Meteorological Society*, *98*(5), 999–1013.
- 340
- 341
- 342 Min, Q., Li, R., Lin, B., Joseph, E., Wang, S., Hu, Y., ... Chang, F. (2008). Evidence of mineral dust altering cloud microphysics and precipitation. *Atmospheric Chemistry and Physics Discussions (ACPD)*, *8*(LF99-8557).
- 343
- 344
- 345 Miyamoto, Y. (2021). Effects of number concentration of cloud condensation nuclei on moist convection formation. *Journal of the Atmospheric Sciences*, *78*(10), 3401–3413.
- 346
- 347 Moore, R., Cerully, K., Bahreini, R., Brock, C., Middlebrook, A., & Nenes, A. (2012). Hygroscopicity and composition of california ccn during summer 2010. *Journal of Geophysical Research: Atmospheres*, *117*(D21).
- 348
- 349
- 350 Morrison, H., van Lier-Walqui, M., Fridlind, A. M., Grabowski, W. W., Harrington, J. Y., Hoose, C., ... others (2020). Confronting the challenge of modeling cloud and precipitation microphysics. *Journal of advances in modeling earth systems*, *12*(8), e2019MS001689.
- 351
- 352
- 353 Novakov, T., & Penner, J. (1993). Large contribution of organic aerosols to cloud-condensation-nuclei concentrations. *Nature*, *365*(6449), 823–826.
- 354
- 355 Qian, Q., Lin, Y., Luo, Y., Zhao, X., Zhao, Z., Luo, Y., & Liu, X. (2018). Sensitivity of a simulated squall line during southern china monsoon rainfall experiment to parameterization of microphysics. *Journal of Geophysical Research: Atmospheres*, *123*(8), 4197–4220.
- 356
- 357
- 358 Riemer, N., Ault, A., West, M., Craig, R., & Curtis, J. (2019). Aerosol mixing state: Measurements, modeling, and impacts. *Reviews of Geophysics*, *57*(2), 187–249.
- 359
- 360 Thompson, G., & Eidhammer, T. (2014). A study of aerosol impacts on clouds and precipitation development in a large winter cyclone. *Journal of the atmospheric sciences*, *71*(10), 3636–3658.
- 361
- 362
- 363 Wong, Y. K., Liu, K. M., Yeung, C., Leung, K. K., & Yu, J. Z. (2022). Measurement report: Characterization and source apportionment of coarse particulate matter in hong kong: insights into the constituents of unidentified mass and source origins in a coastal city in southern china. *Atmospheric Chemistry and Physics*, *22*(7), 5017–5031.
- 364
- 365
- 366
- 367 Yeung, M. C., Lee, B. P., Li, Y. J., & Chan, C. K. (2014). Simultaneous htdma and hr-tof-ams measurements at the hkust supersite in hong kong in 2011. *Journal of Geophysical Research: Atmospheres*, *119*(16), 9864–9883.
- 368
- 369
- 370 Yin, J.-F., Wang, D.-H., Liang, Z.-M., Liu, C.-J., Zhai, G.-Q., & Wang, H. (2018). Numerical study of the role of microphysical latent heating and surface heat fluxes in a severe precipitation event in the warm sector over southern china. *Asia-Pacific Journal of Atmospheric Sciences*, *54*(1), 77–90.
- 371
- 372
- 373
- 374 Yu, S., Luo, Y., Wu, C., Zheng, D., Liu, X., & Xu, W. (2022). Convective and microphysical characteristics of extreme precipitation revealed by multisource observations over the pearl river delta at monsoon coast. *Geophysical Research Letters*, *49*(2), e2021GL097043.
- 375
- 376
- 377 Zhang, S., Liang, Z., Wang, D., & Chen, G. (2022). Nocturnal convection initiation over inland south china during a record-breaking heavy rainfall event. *Monthly Weather Review*.
- 378
- 379 Zhao, X., Lin, Y., Luo, Y., Qian, Q., Liu, X., Liu, X., & Colle, B. A. (2021). A double-moment sbu-ylin cloud microphysics scheme and its impact on a squall line simulation. *Journal of Advances in Modeling Earth Systems*, *13*(11), e2021MS002545.
- 380
- 381

382 Zhou, A., Zhao, K., Lee, W.-C., Ding, Z., Lu, Y., & Huang, H. (2022). Evaluation and modification  
383 of microphysics schemes on the cold pool evolution for a simulated bow echo in southeast  
384 china. *Journal of Geophysical Research: Atmospheres*, 127(2), e2021JD035262.

### 385 **Open Research Section**

386 The Weather Research and Forecast model is publicly available at [https://github.com/wrf-](https://github.com/wrf-model/WRF)  
387 [model/WRF](https://github.com/wrf-model/WRF). We archived the namelist for our simulations and ion data at <https://doi.org/10.5281/zenodo.7401445>.

### 388 **Acknowledgments**

389 The authors thank Yee Ka Wong for sharing the ion observation data. We acknowledge the support  
390 of the Research Grants Council of Hong Kong SAR, China. YW and JF are supported by AoE/E-  
391 603/18, XS by HKUST 16301721.

# Supporting Information for “A Case Study of the Effects of Aerosols on South China Convective Precipitation Forecast”

Yueya Wang<sup>1</sup>, Zijing Zhang<sup>1</sup>, Wing Sze Chow<sup>2</sup>, Zhe Wang<sup>1</sup>, Jian Zhen Yu<sup>1,2</sup>,  
Jimmy Chi-Hung Fung<sup>1,3</sup>, and Xiaoming Shi<sup>1</sup>

<sup>1</sup>Division of Environment and Sustainability, Hong Kong University of Science and Technology, Hong Kong, China

<sup>2</sup>Department of Chemistry, Hong Kong University of Science and Technology, Hong Kong, China

<sup>3</sup>Department of Mathematics, Hong Kong University of Science and Technology, Hong Kong, China

## Contents of this file

1. Tables S1
2. Figures S1 to S4

**Table S1.** WRF configuration for the simulations.

<b>Parameterization</b>	<b>Scheme</b>
Initial and boundary condition	ECMWF Reanalysis V5 (ERA5)
Microphysics	Thomson aerosol-aware
Long-wave radiation	RRTM
Short-wave radiation	RRTM
Surface	Noah Land Surface Model
PBL	ACM2

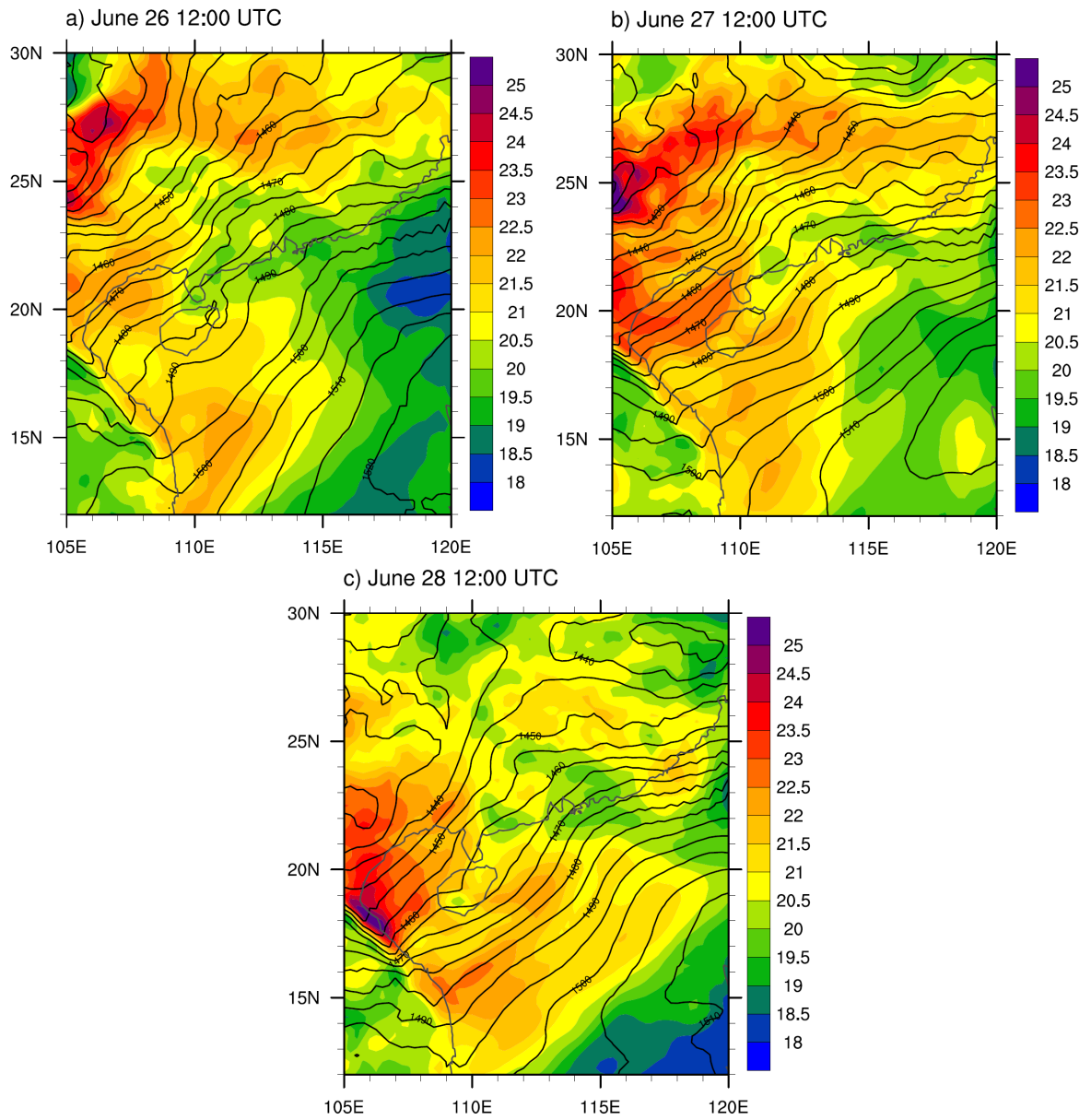


**Figure S1.** The 850 hPa level geopotential height (contours) (m) and temperature (color shading) °C for 12:00 UTC, June 26 to 28, 2021.

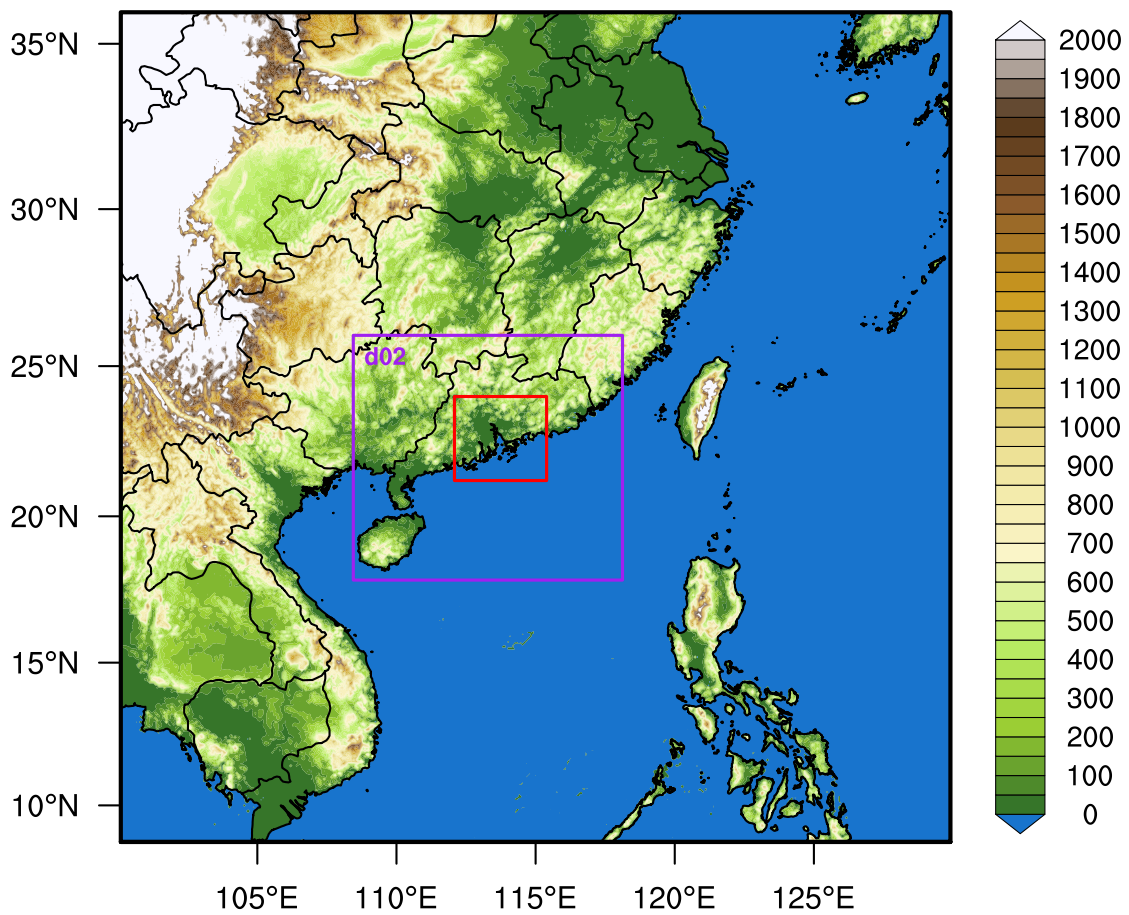


**Figure S2.** The three nested domains with horizontal grid resolutions of 9km, 3km and 1km.

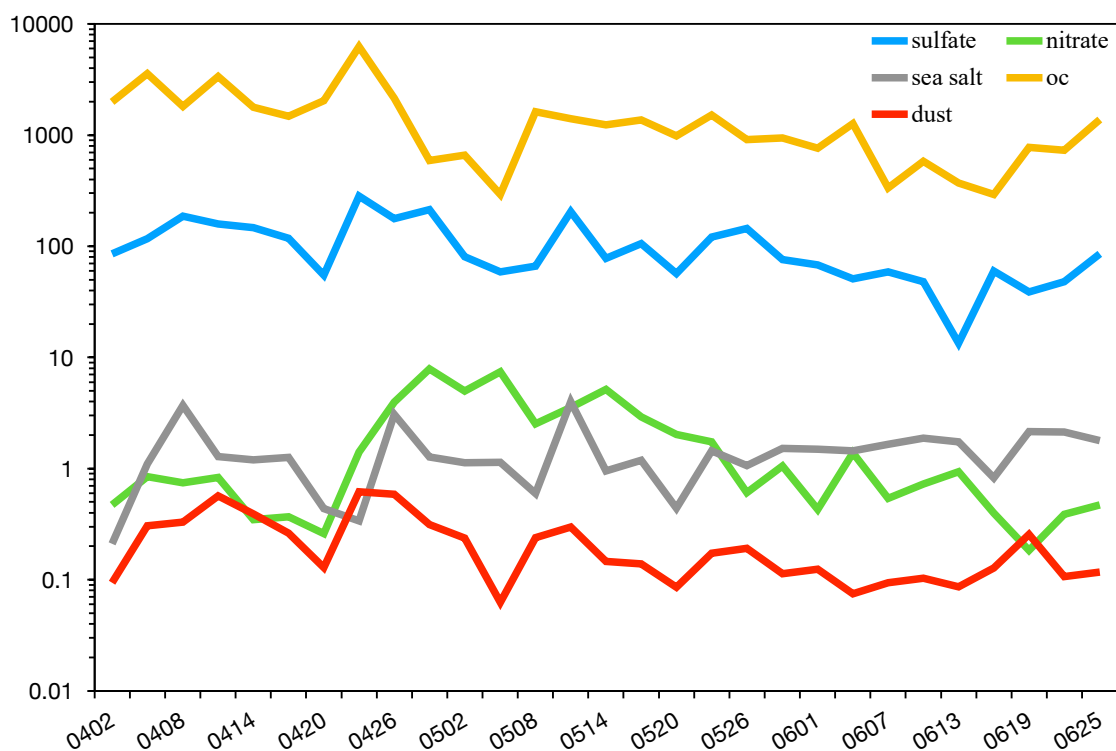


**Figure S3.** The number concentration ( $\text{cm}^{-3}$ ) of the water-friendly aerosols: sulfate (blue), nitrate (green), sea salt (grey), organic carbon (OC) (yellow) and ice-friendly aerosols: dust (red) from 2 April 2020 to 25 June for every three days.

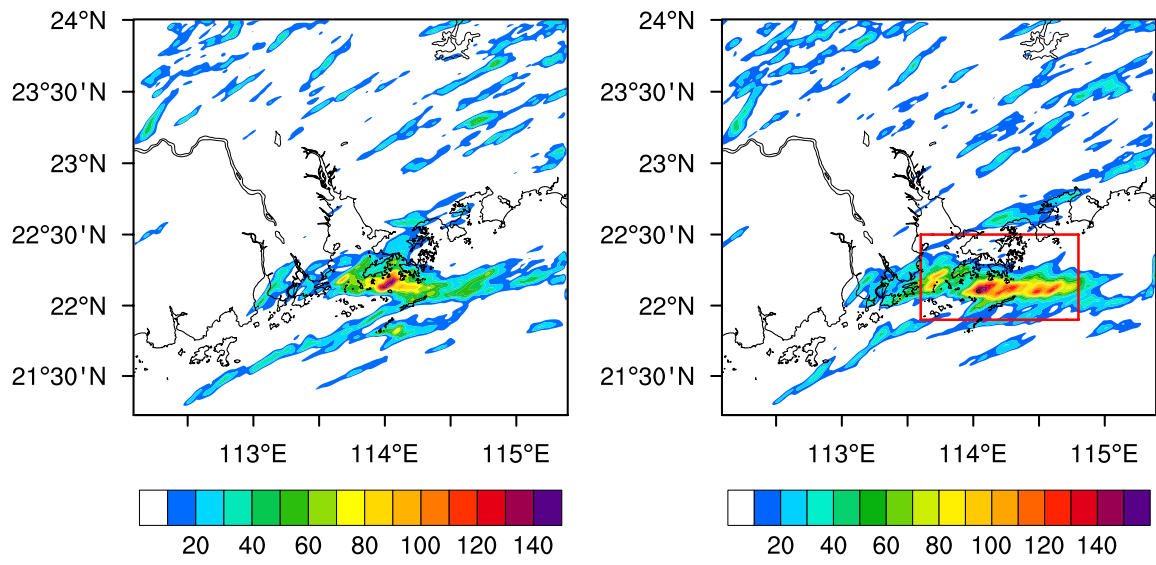


**Figure S4.** Accumulated precipitation from 12 UTC, 27 June to 06 UTC, 28 June: (a) WmaxImax, (b) WminImin. The red box denotes the main precipitation area in the domain.